



UPPSALA
UNIVERSITET

*Digital Comprehensive Summaries of Uppsala Dissertations
from the Faculty of Science and Technology 1495*

Numerical Methods for Darcy Flow Problems with Rough and Uncertain Data

FREDRIK HELLMAN



ACTA
UNIVERSITATIS
UPSALIENSIS
UPPSALA
2017

ISSN 1651-6214
ISBN 978-91-554-9872-6
urn:nbn:se:uu:diva-318589

Dissertation presented at Uppsala University to be publicly examined in ITC 2446, Lägerhyddsvägen 2, Uppsala, Friday, 19 May 2017 at 10:15 for the degree of Doctor of Philosophy. The examination will be conducted in English. Faculty examiner: Professor Robert Scheichl (Department of Mathematical Sciences, University of Bath).

Abstract

Hellman, F. 2017. Numerical Methods for Darcy Flow Problems with Rough and Uncertain Data. *Digital Comprehensive Summaries of Uppsala Dissertations from the Faculty of Science and Technology* 1495. 41 pp. Uppsala: Acta Universitatis Upsaliensis. ISBN 978-91-554-9872-6.

We address two computational challenges for numerical simulations of Darcy flow problems: rough and uncertain data. The rapidly varying and possibly high contrast permeability coefficient for the pressure equation in Darcy flow problems generally leads to irregular solutions, which in turn make standard solution techniques perform poorly. We study methods for numerical homogenization based on localized computations. Regarding the challenge of uncertain data, we consider the problem of forward propagation of uncertainty through a numerical model. More specifically, we consider methods for estimating the failure probability, or a point estimate of the cumulative distribution function (cdf) of a scalar output from the model.

The issue of rough coefficients is discussed in Papers I–III by analyzing three aspects of the localized orthogonal decomposition (LOD) method. In Paper I, we define an interpolation operator that makes the localization error independent of the contrast of the coefficient. The conditions for its applicability are studied. In Paper II, we consider time-dependent coefficients and derive computable error indicators that are used to adaptively update the multiscale space. In Paper III, we derive a priori error bounds for the LOD method based on the Raviart–Thomas finite element.

The topic of uncertain data is discussed in Papers IV–VI. The main contribution is the selective refinement algorithm, proposed in Paper IV for estimating quantiles, and further developed in Paper V for point evaluation of the cdf. Selective refinement makes use of a hierarchy of numerical approximations of the model and exploits computable error bounds for the random model output to reduce the cost complexity. It is applied in combination with Monte Carlo and multilevel Monte Carlo methods to reduce the overall cost. In Paper VI we quantify the gains from applying selective refinement to a two-phase Darcy flow problem.

Keywords: numerical homogenization, multiscale methods, rough coefficients, high contrast coefficients, mixed finite elements, cdf estimation, multilevel Monte Carlo methods, Darcy flow problems

Fredrik Hellman, Department of Information Technology, Division of Scientific Computing, Box 337, Uppsala University, SE-751 05 Uppsala, Sweden.

© Fredrik Hellman 2017

ISSN 1651-6214

ISBN 978-91-554-9872-6

urn:nbn:se:uu:diva-318589 (<http://urn.kb.se/resolve?urn=urn:nbn:se:uu:diva-318589>)

Till pappa

List of papers

This thesis is based on the following papers, which are referred to in the text by their Roman numerals.

- I F. Hellman and A. Målqvist. Contrast independent localization of multiscale problems. *ArXiv e-prints:1610.07398*, 2016. (Submitted)
- II F. Hellman and A. Målqvist. Numerical homogenization of time-dependent diffusion. *ArXiv e-prints:1703.08857*, 2017. (Submitted)
- III F. Hellman, P. Henning, and A. Målqvist. Multiscale mixed finite elements. *Discrete Contin. Dyn. Syst. Ser. S*, 9(5):1269–1298, 2016.
- IV D. Elfverson, D. Estep, F. Hellman, and A. Målqvist. Uncertainty quantification for approximate p-quantiles for physical models with stochastic inputs. *SIAM/ASA J. Uncertain. Quantif.*, 2(1):826–850, 2014.
- V D. Elfverson, F. Hellman, and A. Målqvist. A multilevel Monte Carlo method for computing failure probabilities. *SIAM/ASA J. Uncertain. Quantif.*, 4(1):312–330, 2016.
- VI F. Fagerlund, F. Hellman, A. Målqvist, and A. Niemi. Multilevel Monte Carlo methods for computing failure probability of porous media flow systems. *Advances in Water Resources*, 94:498–509, 2016.

Reprints were made with permission from the publishers.

Contents

1	Introduction	9
2	A two-phase Darcy flow model	12
3	Numerical homogenization	15
3.1	The finite element method and rough coefficients	15
3.2	Multiscale methods	17
3.3	Localized orthogonal decomposition	18
3.4	Contrast independent localization	21
3.5	Adaptive update of the multiscale space	22
3.6	Multiscale mixed finite elements	23
4	Estimating failure probabilities	26
4.1	Monte Carlo	27
4.2	Multilevel Monte Carlo	28
4.3	Selective refinement	29
5	Summary of papers	31
5.1	Paper I	31
5.2	Paper II	31
5.3	Paper III	32
5.4	Paper IV	32
5.5	Paper V	33
5.6	Paper VI	33
6	Sammanfattning på svenska	35
	References	39

1. Introduction

Darcy's law is a model that describes how fluids flow in porous media. It is perhaps the most commonly used model in large-scale computer simulations of subsurface flows, such as spread of pollutants in ground water, flow of water and oil in oil reservoirs for enhanced oil recovery, and flow of brine and carbon dioxide in a saline aquifer for carbon dioxide storage. This thesis studies two major challenges for such computer simulations: (i) that the medium properties are varying with high contrast and at a much finer scale than the scale of the computational domain (rough data), and (ii) that the medium properties are largely unknown (uncertain data). Problems with rough and uncertain data can be found in many other situations, for example in simulations for composite materials. Although many of the results in this thesis are applicable to other problems, we discuss the results in the context of subsurface flows to illustrate one important application.

For Darcy flow problems, the equation for the pressure u often takes the form of an elliptic partial differential equation (PDE)

$$-\nabla \cdot A \nabla u = f,$$

where f are source and sink terms and the coefficient A is related to the permeability. The permeability determines to what extent a fluid can flow through a particular point in the domain, and it can vary significantly over small distances due to local variations in the properties of the rock. It can also vary by large magnitudes, when materials with very different properties occur in the computational domain. If a coefficient has any of these two properties, we call it rough. The finite element method (FEM) is a commonly used method for solving elliptic equations. However, in the case of rapidly varying coefficients, the computational mesh needs to resolve the fine variations of A for the method to yield an accurate solution. A fine mesh makes the resulting linear system of equations very large and a rough coefficient makes it difficult to solve also by iterative methods [7, 12]. To be able to do large-scale simulations, we need memory efficient and parallelizable algorithms.

Numerical homogenization or multiscale methods address the problem of rough coefficients. A commonly recurring strategy is to solve small localized problems, whose solutions are used to construct an upscaled operator or modified basis functions on a coarser mesh, resulting in better coarse scale approximations. In this thesis, we study the localized orthogonal decomposition method (LOD, [27, 29]), which has its roots in the variational multiscale

method (VMS, [24]). LOD is a parallelizable method for constructing a low-dimensional multiscale space based on the coefficient A , with provably good approximation properties. This is in sharp contrast to the standard finite element space, where one always can find a coefficient such that the method converges arbitrarily slowly [5]. Two closely related multiscale methods are the multiscale finite element method [22] and meshfree polyharmonic homogenization [33]. The convergence analysis of the multiscale finite element method, however, relies on periodicity of A . Meshfree polyharmonic homogenization can be applied under milder assumptions, and numerical experiments show that localization is possible with maintained accuracy for this method as well.

We focus on three aspects of the LOD. One aspect is high contrast coefficients, i.e. when the ratio between largest and smallest value of A is large. The contrast enters the error bounds of the standard LOD as a constant and reduces the possibility for localization. We make the simplifying assumption that A is equal to either α or 1 in each point, which allows us to make a geometrical interpretation of the coefficient. We propose a modification of the LOD for contrast independent localization. Another aspect is time-varying coefficients that occur in, for example, time-dependent two-phase Darcy flow problems. Here we construct an initial multiscale space and derive error indicators that can tell when and what parts of the multiscale space to update to keep the error small, as we iterate in time. Finally, we apply the LOD to mixed finite elements, more specifically the Raviart–Thomas finite element. We derive a priori error bounds independent of fine scale variations and obtain a solution that is locally conservative.

The coefficient A in the pressure equation above is typically not only rough, but also uncertain. This has motivated us to develop and analyze methods for forward propagation of uncertainty. The setting is general. We consider an output X from a model with random input ω , and we are interested in estimating the failure probability $p = F(y)$, where F is the cumulative distribution function of X . In other words, the quantity of interest X indicates a failure if $X \leq y$ and p is the probability for this to happen. Methods for this kind of problems include those constructing representations of X in the stochastic space, e.g. first/second order reliability methods (FORM/SORM) [26] and surrogate-based methods (e.g. [28]). The former are not expected to perform well if there is no known normal state from which a limit point for failure can be determined. The latter suffer from the curse of dimensionality. This can be an issue for subsurface flow problems where the random input typically is a spatial random field of high stochastic dimension. There are also sample based methods specifically constructed for computing failure probabilities, e.g. subset simulation [2, 41], where Markov Chain Monte Carlo techniques are used to generate samples concentrated to the failure event.

In this thesis, we consider sample based methods for stochastic integration. We focus on Monte Carlo and multilevel Monte Carlo [16] methods that are in-

dependent of the representation of the random input. However, the results are applicable also to quasi-Monte Carlo methods, lattice rules and sparse grids, if regularity allows for any gain in using them. We consider the typical case that only numerical approximations of X are available and that we are able to compute approximations X_ℓ for which the error $|X - X_\ell|$ decreases exponentially with ℓ . We use computable error bounds to find subsets of realizations to compute at lower levels of approximation and thus achieve improved computational cost complexity compared to the standard Monte Carlo method and the multilevel Monte Carlo method

The subsequent chapters give a more detailed summary of the papers included in this thesis. Chapter 2 introduces a two-phase Darcy flow model that is used in many numerical experiments and examples in the included papers. Chapter 3 discusses the topic of numerical homogenization that is covered by Papers I–III, and Chapter 4 reviews the work on failure probability estimation found in Papers IV–VI.

2. A two-phase Darcy flow model

Gravel, sandstone, limestone, and packed coffee powder are a few examples of porous media. A porous medium consists of a solid material called matrix, with a network of cavities known as pores. We are interested in simulating the flow of fluids within the pores. In many cases there are several immiscible fluids sharing the pore space. In the context of porous media flow, they are called phases. We call oil and water in sandstone a two-phase system since the two fluids do not mix, although both of them are liquids. Air and water in packed coffee powder is another example of a two-phase system. We will only consider single- or two-phase systems in this thesis. In a two-phase system, the phase that is most strongly attracted to the solid matrix is called the wetting phase and the other phase is called the non-wetting phase. Figure 2.1 gives an

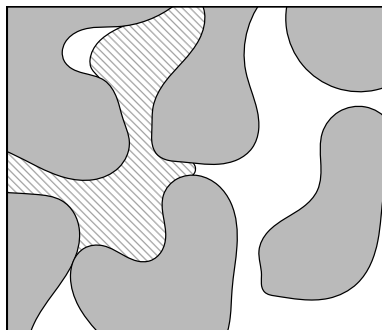


Figure 2.1. A cross section of a porous medium with two phases filling the pore space. Gray, white, and striped fields represent the solid, wetting phase, and non-wetting phase, respectively.

illustration of a cross section of a porous medium depicting pore space, solid and the two phases with a sharp interface.

While fluid flow through a porous medium can be modeled using the first principle Navier–Stokes equations or a network model at microscopic level, this thesis focuses on the macroscopic Darcy’s law. In a macroscopic model, medium properties and state variables need to be averaged over, or upscaled to, a representative elementary volume (REV). A point in the macroscopic model corresponds to averages or upscaled quantities over an REV located at the point in question. New variables that were not present in the microscopic model enter the model. Since several phases can occupy the same REV, a saturation variable $0 \leq s_\beta \leq 1$ is introduced for each phase β , stating the fraction

of the pore volume that is occupied by phase β . This means that at the macroscopic level we do not recognize the sharp interface between phases. Another upscaled quantity is hydraulic conductivity, which specifies how easily a phase flows through the pores in presence of a pressure gradient. The hydraulic conductivity depends on the viscosity of the fluid, the pore sizes and connectivity between pores, and whether there are other phases present that block the way. Darcy's law reads, for phases $\beta = n, w$ (non-wetting and wetting, respectively) in domain Ω ,

$$\boldsymbol{\sigma}_\beta = -\frac{k_{r\beta}(s_\beta)}{\mu_\beta} K(\nabla u_\beta - \rho_\beta \mathbf{g}), \quad (2.1)$$

where $\boldsymbol{\sigma}_\beta$ is Darcy (volumetric) flux, $k_{r\beta}$ is relative permeability, μ_β is dynamic viscosity, s_β is saturation, K is intrinsic permeability, u_β is pressure, ρ_β is fluid density, and \mathbf{g} is gravitational acceleration. All quantities above are considered over an REV. The intrinsic permeability (or just the permeability) K reflects to what degree the pore structure in the REV allows for fluid flow and is independent of the fluid properties and the saturation. Relative permeability $0 \leq k_{r\beta}(s_\beta) \leq 1$ is a nonlinear function of the saturation which in product with intrinsic permeability forms the effective permeability. It models the reduction in effective permeability when the pore space is blocked by the presence of the other phase.

We proceed by presenting single- and two-phase flow models under a number of simplifying assumptions to reach to the challenging enough elliptic pressure equation. We assume that the fluids are immiscible and that there is no mass exchange between the phases. Then we have mass conservation for each phase,

$$\phi \frac{\partial s_\beta}{\partial t} + \nabla \cdot \boldsymbol{\sigma}_\beta = f_\beta, \quad (2.2)$$

where ϕ is porosity (pore space fraction of REV) and f_β is a source or sink term. Here we also assumed incompressibility of the fluids and solid. In addition to (2.1) and (2.2) we define a relation between the phase pressures by a capillary pressure curve $p_c(s_w) = u_n - u_w$ and further let $s_w + s_n = 1$ to close the system. In a single-phase system we omit the subscript β , and use $s \equiv 1$ to make (2.1) and (2.2) form the elliptic pressure equation,

$$-\nabla \cdot A \nabla u = f, \quad (2.3)$$

where $A = \frac{k_r}{\mu} K$ (the gravitational force was discarded for simplicity). For a two-phase system with no capillary pressure, we can sum the equations (2.1) and (2.2) over both phases to get (2.3) with $u = u_n = u_w$ (no capillary pressure), $A = \lambda(s_w)K$, where $\lambda(s_w) = \left(\frac{k_{rw}(s_w)}{\mu_w} + \frac{k_{rn}(1-s_w)}{\mu_n} \right)$ is the total mobility function, and $f = f_w + f_n$.

In view of this model, the motivation for the topics in this thesis is the rough and uncertain intrinsic permeability K . A rough K appears when the compu-

tational domain Ω is of reservoir or aquifer scale (1–10 km), while the permeability K varies at a much smaller scale (10 m). The contrast problem appears when highly permeable areas and less permeable areas coexist, for example when channel structures are present. This topic is discussed next in Chapter 3. Uncertainty in K comes from the difficulties in measuring the permeability, since direct samples of K are typically available only along boreholes. We take a probabilistic approach to this uncertainty. Geostatistical models can be used to generate possible realizations of K that can be used as inputs to the methods discussed in Chapter 4.

3. Numerical homogenization

In this chapter, we consider numerical methods for Poisson's equation in (2.3) when the coefficient A is rough in the sense that it is varying rapidly in space, possibly in combination with high contrast. We let Ω denote a polygonal domain in \mathbb{R}^d ($d = 1, 2$, or 3) in which the equation is posed. Assuming that A is differentiable, we say that A is rapidly varying if $\|\nabla A\|_{L^\infty(\Omega)} \sim \varepsilon^{-1}$ with $\varepsilon \ll 1$, and that it has high contrast if $\frac{\sup_{\Omega} A}{\inf_{\Omega} A}$ is large. For such coefficients, the solution is generally irregular and standard numerical techniques for (2.3) perform poorly. As we will soon see, the standard \mathcal{P}_1 finite element discretization generally requires a mesh with element diameter $h \leq \varepsilon$ to yield accurate solutions [4]. The resulting linear system is also challenging to solve. The multigrid method, for instance, which performs well for many problems, converges slowly for rapidly varying coefficients in general [12]. This chapter summarizes the work in Papers I–III.

3.1 The finite element method and rough coefficients

To illustrate the problem of a rapidly varying coefficient, we study the 1D equation (from [34])

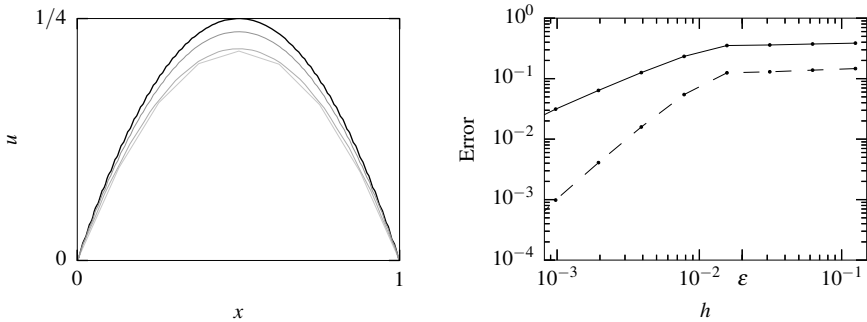
$$-(Au_x)_x = 1, \quad \text{for } 0 \leq x \leq 1,$$

with $A = (2 - \cos(2\pi x\varepsilon^{-1}))^{-1}$ and boundary conditions $u(0) = u(1) = 1$. The solution is

$$u = x - x^2 - \frac{\varepsilon}{2\pi} \left(\frac{1}{2} \sin(2\pi x\varepsilon^{-1}) - x \sin(2\pi x\varepsilon^{-1}) - \frac{\varepsilon}{2\pi} \cos(2\pi x\varepsilon^{-1}) + \frac{\varepsilon}{2\pi} \right). \quad (3.1)$$

We note that the coefficient A is rapidly varying at scale ε , and that $|u_{xx}| \sim \varepsilon^{-1}$. We let $\varepsilon = 0.02$ and use the \mathcal{P}_1 finite element (globally continuous, piecewise linear functions) on a sequence of meshes with element size h to solve the problem. We get the solutions shown in Figure 3.1 and see clearly that the fine scale variations need to be resolved by the mesh (i.e. $h \leq \varepsilon$) to get accurate solutions.

In the remainder of this chapter, we consider a weak formulation of (2.3) and assume only that $A \in L^\infty(\Omega)$. We impose homogeneous Dirichlet and Neumann boundary conditions on Γ_D (non-empty) and $\Gamma_N \subset \partial\Omega$, respectively. We introduce the Sobolev space $H^1(\Omega)$ of functions with L^2 -integrable weak



(a) The thick upper-most line is the true solution. Solutions for mesh sizes $h = 8, 64$, and 128 are plotted in gray.

(b) Relative errors of FEM approximation in energy norm (solid line) and L^2 -norm (dashed line) as functions of h .

Figure 3.1. FEM approximations of 1D problem with rapidly varying coefficient.

first derivatives over Ω and define $V = \{v \in H^1(\Omega) : v|_{\Gamma_D} = 0\}$ where the specification of boundary values is to be interpreted in the sense of traces. After multiplying by a test function from V and integrating by parts, we obtain the weak formulation, find $u \in V$, such that for all $v \in V$,

$$a(u, v) = (f, v), \quad (3.2)$$

where $a(u, v) = \int_{\Omega} A \nabla u \cdot \nabla v$ and $(f, v) = \int_{\Omega} f v$. In our particular case, we assume that $0 < \alpha \leq A \leq 1$, so that a is bounded and coercive on V , and that f is a bounded linear functional on V . Then, by the Lax–Milgram theorem this problem has a unique solution $u \in V$. The upper bound 1 of A is no limitation, since this can be obtained by rescaling A and f .

Coercivity and boundedness are inherited to subspaces. This makes it very easy to construct a discretization of (3.2). In the case of the finite element method (see e.g. [8, 10]), this is done by partitioning the domain Ω into a set of elements \mathcal{T}_h . For simplicity, we consider quasi-uniform families of partitions into simplices, where $\rho^{-1}h \leq \text{diam}(T) \leq h$ for all $T \in \mathcal{T}_h$ and a constant ρ independent of h . We then construct the conforming \mathcal{P}_1 finite element spaces, parametrized by mesh size h ,

$$V_h = \{v \in V : v|_T \in \mathcal{P}_1 \text{ for all } T \in \mathcal{T}_h\},$$

where \mathcal{P}_1 contains the polynomials of degree at most 1. Replacing V with V_h in (3.2) gives the discrete Ritz–Galerkin problem, find $u_h \in V_h$, such that for all $v_h \in V_h$,

$$a(u_h, v_h) = (f, v_h). \quad (3.3)$$

Galerkin-orthogonality $a(u - u_h, v_h) = 0$ yields the best-approximation result (Céa’s Lemma)

$$\|u - u_h\| \leq \|u - v_h\|, \quad (3.4)$$

where $\|v\|^2 = a(v, v)$ denotes the energy norm.

To get an a priori error bound for $u - u_h$ in terms of h , we assume sufficient smoothness of u and regularity of the mesh. More specifically we assume that $u \in H^2(\Omega)$, so that the nodal interpolation $\mathcal{I}_h^{\text{nodal}}u$ of u onto V_H is well-defined, and that ρ (in addition to being a quasi-uniformity parameter) is a mesh regularity parameter. Then we substitute the arbitrary v_h in Céa's Lemma by $\mathcal{I}_h^{\text{nodal}}u$, and obtain by interpolation estimates (see e.g. [8]) that

$$\|u - u_h\| \leq \|u - \mathcal{I}_h^{\text{nodal}}u\| \leq |u - \mathcal{I}_h^{\text{nodal}}u|_{H^1(\Omega)} \leq Ch|u|_{H^2(\Omega)},$$

where the constant C depends on ρ . We observe that we need $h \leq |u|_{H^2(\Omega)}$ for accurate solutions with the Ritz–Galerkin finite element method. In the 1D example presented previously in this chapter, we observed that variations of order ε in A can cause the second derivative of the solution to be of order ε^{-1} . Thus, we have seen that the standard finite element method generally requires resolving meshes to obtain accurate solutions for problems with rapidly varying coefficient.

One interpretation of these observations in combination with Céa's Lemma (3.4) is that the space V_h has poor approximation properties for problems with rapidly varying coefficients. All works related to rough coefficients in this thesis are about constructing a low-dimensional space (multiscale space) with good approximation properties, in the sense that a good approximation can be found in the space and will be the solution guaranteed by Céa's Lemma, also when A is rapidly varying. This is the symmetric (Galerkin) version of localized orthogonal decomposition (LOD) [29]. We do, however, also consider nonsymmetric Petrov–Galerkin methods where the multiscale space is used as either trial and test space, where similar quasi-optimal approximation results hold on the basis of inf-sup stability.

3.2 Multiscale methods

If we are interested in a good L^2 -approximation of the solution in the 1D example in the previous section, it is possible to obtain this by replacing the coefficient by its harmonic average $\bar{A}|_T = |T| (\int_T A^{-1})^{-1}$ on each element T . Then the pre-asymptotic regime in the L^2 -norm of the error for $h \geq \varepsilon$ is removed [4] and accurate solutions can be obtained also for meshes not resolving the variations. This result can be intuitively explained by thinking of the problem in terms of the steady state heat equation, where A is heat conductivity. Obviously, in 1D, there is a bottle-neck effect when the heat conductivity is low in some parts of the line. However, in an arithmetic average (as is in fact performed in the standard method), the average is in the order of magnitude of the larger values, while in a harmonic average, the lower values dominate the average, modeling the bottle-neck effect correctly. Unfortunately, this particular averaging does not generalize to higher dimensions. This can easily be

seen by considering isolated islands of low conducting materials in 2D, which should not cause a bottle-neck effect.

Asymptotic homogenization [6] is a theoretical framework for constructing homogenized coefficients for periodic coefficients. In this framework, we consider a sequence of PDEs with coefficient $A_\varepsilon = A_\varepsilon(\frac{x}{\varepsilon})$ where $A_\varepsilon(y)$ is 1-periodic in its argument y . For such problems, it is possible to find an effective (homogenized) coefficient A_0 in the limit $\varepsilon \rightarrow 0$. The multiscale finite element method [22] is a method for numerical homogenization inspired by asymptotic homogenization. It solves localized problems on a fine mesh resolving the coefficient (i.e. $h \leq \varepsilon$) on patches around the basis functions from a finite element space on a coarser mesh \mathcal{T}_H ($H > h$). The fine-scale computations are used to modify the coarse basis functions and capture the fine scale features of the coefficient. Convergence for periodic coefficients with non-resolving coarse meshes $H \geq \varepsilon$ is shown in [23] in the limit $\varepsilon \rightarrow 0$. However, in many realistic settings, for instance in the modeling of permeability for subsurface flow [14], there is no clear scale ε for the variations, and the coefficient is typically not periodic.

The multiscale methods discussed in this thesis are based on ideas from the variational multiscale method (VMS) [24, 25]. We introduce a family of coarse meshes \mathcal{T}_H and corresponding \mathcal{P}_1 finite element spaces V_H . A fine space V^f is chosen, such that the full space V can be decomposed into $V = V_H \oplus V^f$. In the VMS, we use the linear independence of $v_H \in V_H$ and $v^f \in V^f$, and test (3.2) with v_H and v^f separately. The trial function can also be decomposed into $u = u_H + u^f$. The resulting system is,

$$\begin{aligned} a(u_H + u^f, v_H) &= (f, v_H), \\ a(u^f, v^f) &= (f, v^f) - a(u_H, v^f). \end{aligned} \tag{3.5}$$

We note that the fine scale part u^f of the solution is driven by the residual of the coarse scale. The discussions in e.g. [24, 25] go further by introducing and investigating the properties of a fine-scale Green's function, for example by relating the resulting numerical methods to stabilization schemes. In the localized orthogonal decomposition method, we deviate here and consider the fine scale equation in (3.5) as a basis for the definition of correctors used to construct a multiscale space.

3.3 Localized orthogonal decomposition

In the LOD [27, 29], we specify $V^f = \ker \mathcal{I}_H$ to be the kernel of a projective interpolation operator $\mathcal{I}_H : V \rightarrow V_H$ satisfying the approximability and stability property

$$H^{-1} \|v - \mathcal{I}_H v\|_{L^2(T)} + \|\nabla(v - \mathcal{I}_H v)\|_{L^2(T)} \leq C \|\nabla v\|_{L^2(U(T))},$$

where $U(T)$ is the union of all elements adjacent (by nodes) to T . A Clément type [11] or Scott–Zhang type [37] interpolation operator is typically chosen. The nodal interpolation operator is not defined in V in general. In a practical implementation, the space V is replaced by a finite-dimensional space V_h based on a fine mesh \mathcal{T}_h with $h \leq \varepsilon$, and the nodal interpolation operator can be used, however, this reduces the accuracy [29].

For the remainder of this section, we will neglect the fine scale contribution of the right hand side f in (3.5), and only consider fine scale corrections from the coarse part of the solution. We define the global corrector operator $\mathcal{Q} : V \rightarrow V^f$

$$a(\mathcal{Q}v, v^f) = a(v, v^f), \quad (3.6)$$

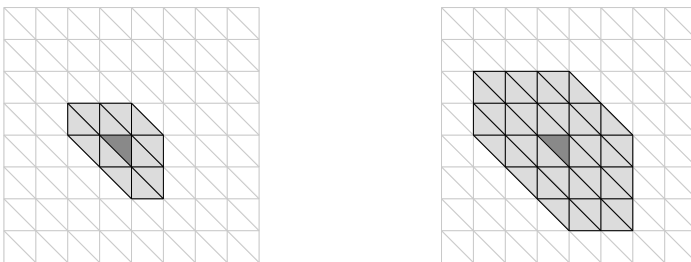
and define a low-dimensional multiscale space $V^{\text{ms}} = \{v - \mathcal{Q}v : v \in V_H\}$. We note that $a(v^{\text{ms}}, v^f) = 0$ for all $v^{\text{ms}} \in V^{\text{ms}}$ and $v^f \in V^f$, i.e. that V^{ms} is orthogonal to V^f in the scalar product a . The non-localized symmetric Galerkin formulation of LOD reads, find $u^{\text{ms}} \in V^{\text{ms}}$, such that for all $v^{\text{ms}} \in V^{\text{ms}}$,

$$a(u^{\text{ms}}, v^{\text{ms}}) = (f, v^{\text{ms}}).$$

Galerkin orthogonality gives $a(u - u^{\text{ms}}, v^{\text{ms}}) = 0$, so that $u - u^{\text{ms}} \in V^f$, i.e. the error is in the kernel space of \mathcal{I}_H . This gives the error bound

$$\| \|u - u^{\text{ms}}\| \|^2 = (f, u - u^{\text{ms}} - \mathcal{I}_H(u - u^{\text{ms}})) \leq C\alpha^{-1/2}H \|f\|_{L^2(\Omega)} \| \|u - u^{\text{ms}}\| \|,$$

where C depends only on the interpolation stability and mesh regularity. We note that neither the regularity of u nor the rapid variations in A appear in the bound.



(a) One coarse layer patch, $k = 1$.

(b) Two coarse layer patch, $k = 2$.

Figure 3.2. Illustration of patches. T is dark gray and $U_k(T)$ is light gray.

Computing a localized approximation of \mathcal{Q} is central to the efficiency of the LOD method. We decompose the corrector $\mathcal{Q} = \sum_T \mathcal{Q}_T$ into element correctors $\mathcal{Q}_T : V \rightarrow V^f$,

$$a(\mathcal{Q}_T v, v^f) = a(v, v^f)_T, \quad (3.7)$$

where $a(u, v)_T = \int_T A \nabla u \cdot \nabla v$. Localization is done by computing approximations of the element correctors \mathcal{Q}_T on patches around T . Exponential decay of \mathcal{Q}_T with distance from T allows for localization with small sacrifice in accuracy.

We define element patches $U_k(\omega) \subset \Omega$, for $\omega \subset \Omega$ (typically ω is an element), where $0 \leq k \in \mathbb{N}$. With trivial case $U_0(\omega) = \omega$, $U_k(\omega)$ (a k -layer element patch around ω) is defined by the recursive relation

$$U_{k+1}(\omega) = \bigcup \{T' \in \mathcal{T}_H : \overline{U_k(\omega)} \cap \overline{T'} \neq \emptyset\}.$$

See Figure 3.2 for examples of element patches. Let $V^f(U_k(T)) = \{v \in V^f : v|_{\Omega \setminus U_k(T)} = 0\}$ be the space of fine functions that are zero outside the element patches. Then we define localized element correctors $\mathcal{Q}_{k,T} : V \rightarrow V^f(U_k(T))$ by

$$a(\mathcal{Q}_{k,T}v, v^f) = a(v, v^f)_T, \quad (3.8)$$

for all $v^f \in V^f(U_k(T))$. We get the localized corrector $\mathcal{Q}_k = \sum_T \mathcal{Q}_{k,T}$. It was shown in [21, 29] that

$$\|\mathcal{Q}v - \mathcal{Q}_k v\|^2 \leq Ck^d \theta^{2k} \sum_T \|\mathcal{Q}_T v\|^2, \quad (3.9)$$

where $0 < \theta < 1$ and C depend on the contrast α^{-1} , but not on H , k or rapid variations in A . This inequality shows that the corrector localization error decays exponentially with the patch size parameter k .

A localized multiscale space $V_k^{\text{ms}} = \{v_H - \mathcal{Q}_k v_H : v \in V_H\}$ can now be constructed. This is relatively cheap to compute and the computations are parallelizable over coarse elements T . In practice, one computes $\phi_x - \sum_T \mathcal{Q}_{k,T} \phi_x$ for every basis function $\phi_x \in V_H$. Since each T only overlaps the support of a few basis functions, and each application of $\mathcal{Q}_{k,T}$ is a problem posed only on a patch $U_k(T)$, the computational cost is small. The localized symmetric Galerkin formulation of LOD reads, find $u_k^{\text{ms}} \in V_k^{\text{ms}}$, such that for all $v_k^{\text{ms}} \in V_k^{\text{ms}}$,

$$a(u_k^{\text{ms}}, v_k^{\text{ms}}) = (f, v_k^{\text{ms}}).$$

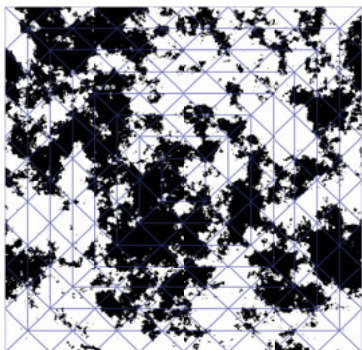
Using the exponential decay of the correctors, the following error bound for $u - u_k^{\text{ms}}$ can be derived (see e.g. [21])

$$\|u - u_k^{\text{ms}}\| \leq C(H + k^{d/2} \theta^k) \|f\|_{L^2(\Omega)},$$

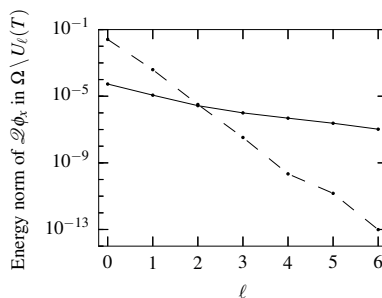
where C is independent of H , k and the regularity of u . It does, however, depend on the contrast α^{-1} for general interpolation operators. By letting the patch size scale with H according to $k \approx |\log(H)|$, we get a solution u_k^{ms} with error proportional to H , independent of the regularity of u and the fine-scale variations in A .

3.4 Contrast independent localization

In many applications, the contrast α^{-1} can be in the order of 10^2 – 10^5 . This happens for Darcy flow problems in porous media with very different permeability in different parts of the domain, for example when channel structures are present. The result (3.9) on the exponential decay of the localization error presented in the previous section depends on the contrast. In many test cases with high contrast, for example when A is defined on a fine mesh with an independent uniformly distributed value between α and 1 in each element, the constant θ is independent of, or only weakly dependent on the contrast. However, it is possible to construct examples when the corrector decay is highly contrast dependent. Consider the coefficient on $\Omega = [0, 1]^2$ in Figure 3.3. For basis function ϕ_x with $x = (0.5, 0.5)$, the plot to the right shows the decay of the energy norm of the basis corrector $\mathcal{Q}\phi_x$ in the annulus $\Omega \setminus U_\ell(\text{supp } \phi_x)$ as a function of ℓ . The solid line corresponds to a Clément type interpolation operator with no special adjustments for high contrast, and we can see that the decay is slow. The dashed line corresponds to an operator proposed in Paper I, whose decay is contrast independent.



(a) Coefficient A , and a coarse mesh. White indicates $A = 10^{-5}$ and black $A = 1$. The basis function ϕ_x corresponds to the midpoint.



(b) Energy norm of $\mathcal{Q}\phi_x$ in the annulus $\Omega \setminus U_\ell(\text{supp } \phi_x)$ for two different \mathcal{I}_H . The solid line is a standard Clément type operator, and the dashed line is the operator proposed in Paper I.

Figure 3.3. Illustration of slow corrector decay for a high contrast coefficient.

The high contrast problem for the LOD method for continuous coefficients has been discussed previously in [35], where A -weighted interpolation operators are used and shown to give contrast independent decay under assumptions of quasi-monotonicity of A on all node patches. In the work presented in Paper I we limit ourselves to the case when A takes one of only two possible values, α or 1, in every point. We partition Ω into two disjoint subdomains Ω^1 and Ω^α . These subdomains are defined by the values of A , so that $A|_{\Omega^\alpha} = \alpha$ and $A|_{\Omega^1} = 1$. This allows for a geometrical interpretation of the coefficient in terms of the subdomains Ω^α and Ω^1 . We make the observation that all numer-

ical inaccuracies possibly stemming from complex geometries of Ω^α and Ω^1 (for example high permeable channel structures or low conducting inclusions) in the limit $\alpha \rightarrow 0$ are contained in the constant α^{-1} in the classical LOD error bounds. This constant is the only information about the geometry available in the error analysis.

The reason why the contrast appears in the error analysis of the standard LOD is bounds of the kind

$$\|A^{1/2}v^f\|_{L^2(T)} \leq \|v^f - \mathcal{I}_H v^f\|_{L^2(T)} \leq C\alpha^{-1/2}H\|A^{1/2}\nabla v^f\|_{L^2(U(T))}, \quad (3.10)$$

for fine scale functions $v^f \in V^f$. The main idea in Paper I is to split the integral to the left in (3.10) over subdomains Ω^1 and Ω^α ,

$$\|A^{1/2}v^f\|_{L^2(T)}^2 = \|v^f\|_{L^2(\Omega^1 \cap T)}^2 + \alpha\|v^f\|_{L^2(\Omega^\alpha \cap T)}^2.$$

For the second term, we do as in (3.10), i.e. change norm and use the interpolation error, since α will cancel α^{-1} . For the first term, however, we have a problem with the standard interpolation error bound spreading outside Ω^1 and into Ω^α . This makes the constant α^{-1} appear when changing back to energy norm. Instead, we construct an interpolation operator \mathcal{I}_H that admits a Poincaré type inequality over only Ω^1 in the fine space $V^f = \ker \mathcal{I}_H$,

$$\|v^f\|_{L^2(\Omega^1 \cap T)} \leq CH\|\nabla v^f\|_{L^2(\Omega^1 \cap U_\ell(T))}, \quad (3.11)$$

with C independent of α^{-1} and an integer $\ell \geq 1$ that depends on \mathcal{I}_H and the geometry of Ω^1 . In order to obtain this inequality, the geometry of Ω^1 is considered when defining \mathcal{I}_H : The nodal variables for a subset of nodes are defined as integrals exclusively over Ω^1 . If this is done for all disjoint inclusions in Ω^1 with nodes placed frequently enough, it is possible to prove the inequality in (3.11). This puts some conditions on the placement of coarse nodes in relation to the geometry of Ω^1 . Using this technique, we can obtain a bound

$$\|A^{1/2}v^f\|_{L^2(T)} \leq \|v^f - \mathcal{I}_H v^f\|_{L^2(T)} \leq CH\|A^{1/2}\nabla v^f\|_{L^2(U_\ell(T))},$$

with C independent of the contrast. From this we can derive an exponential decay bound as in (3.9), but with constants C and θ independent of α^{-1} .

3.5 Adaptive update of the multiscale space

For problems with several elliptic equations with similar coefficients A , it is natural to try to reuse a multiscale space constructed for one of the coefficients.

One example of this situation is sample based stochastic integration for defects in composite materials, where coefficients A (corresponding to defect

materials) are sampled by randomly perturbing a base coefficient of a non-defect reference material. If the defects are spatially localized, the multiscale spaces for the two coefficients are similar and many of the correctors computed for the multiscale space for the base coefficient can be reused.

Another example appears in two-phase Darcy flow problems in the formulation given in Chapter 2. In a situation where one fluid is injected into a reservoir filled with another fluid, the saturation s forms a plume sweeping through the domain. The coefficient $A = \lambda(s)K$ depends on s through the scalar total mobility function λ . A pressure equation needs to be solved in every time step while the plume is advancing, changing the coefficient A as time passes. The largest changes occur at the plume front. Again, we can hope to reuse many of the correctors already computed for the coefficient in the previous time steps.

In Paper II, we consider the more general setting where each element corrector has been computed (by (3.8)) using a so called lagging coefficient \tilde{A}_T instead of the true coefficient A . We derive computable error indicators for each element corrector, and compare them with a tolerance TOL to determine whether to recompute the element corrector or not. If we denote by $\tilde{Q}_{k,T}$ the element corrector that has previously been computed (lagging corrector), the error indicator for element T is

$$e_{u,T} = \max_{\substack{w|_T: w \in V_H, \\ \|A^{1/2}\nabla w\|_{L^2(T)}=1}} \|(\tilde{A}_T - A)A^{-1/2}(\chi_T \nabla w - \nabla \tilde{Q}_{k,T} w)\|_{L^2(U_k(T))}.$$

where χ_T is the indicator function for element T . This corresponds to the square root of the maximum eigenvalue in a low-dimensional generalized eigenvalue problem (a 3×3 matrix for tetrahedral elements in 3D) and is thus cheap to compute. This quantity bounds the error in the lagging corrector $\tilde{Q}_{k,T}$ by

$$\|Q_{k,T} v - \tilde{Q}_{k,T} v\| \leq e_{u,T} \|A^{1/2} \nabla v\|_{L^2(T)}, \quad \text{for all } v \in V_H.$$

In particular, we note that if we recompute the element corrector with the true coefficient A , so that $\tilde{A}_T = A$, then the both the error $\|Q_{k,T} v - \tilde{Q}_{k,T} v\|$ and $e_{u,T}$ are zero. The error indicators are used in a Petrov–Galerkin formulation of the LOD. The full error from using lagging coefficients scales with $k^{d/2}(\max_T e_{u,T})\|f\|_{L^2(\Omega)}$. Keeping $e_{u,T}$ below a tolerance is done by recomputing all element correctors (using the true coefficient) on elements T for which $e_{u,T} \geq \text{TOL}$ for some predetermined value of TOL.

3.6 Multiscale mixed finite elements

The coupled system of pressure (2.1) and saturation (2.2) equations is often solved by sequential splitting techniques, where the pressure equation is solved based on the saturation from the previous time step, and the saturation

equation is solved using the fluxes obtained from the pressure equation at the current time step. This procedure is iterated in time to simulate the coupled process. Locally conservative fluxes are generally necessary for stable and accurate solutions to discontinuous Galerkin or finite volume schemes used to solve the advective transport equation (see e.g. [40] for a confirming counter example). In the mixed form of (2.3) we seek the flux $\boldsymbol{\sigma}$ and pressure u , such that

$$\begin{aligned} A^{-1}\boldsymbol{\sigma} + \nabla u &= 0, \\ \nabla \cdot \boldsymbol{\sigma} &= f. \end{aligned} \tag{3.12}$$

The flux $\boldsymbol{\sigma}$ is an explicit unknown that will be locally conservative if choosing the discretization properly. The Raviart–Thomas finite element [31, 36] is one of the most common discretizations of the flux space and it gives locally conservative fluxes by construction. In Paper III, we derive an a priori error bound for an LOD method for the mixed problem (3.12) yielding locally conservative fluxes on the coarse mesh (and the fine mesh if right hand side correction is performed).

The weak formulation of the mixed problem uses the spaces $H(\text{div}, \Omega)$ and $H_0(\text{div}, \Omega) = \{\mathbf{v} \in H(\text{div}, \Omega) : \mathbf{v} \cdot \mathbf{n}|_{\partial\Omega} = 0\}$ where \mathbf{n} is the outward facing boundary normal. The weak formulation of a homogeneous Neumann problem reads, find $\boldsymbol{\sigma} \in H_0(\text{div}, \Omega)$, and $u \in L^2(\Omega)/\mathbb{R}$, such that

$$\begin{aligned} (A^{-1}\boldsymbol{\sigma}, \mathbf{v}) - (\nabla \cdot \mathbf{v}, u) &= 0, \\ (\nabla \cdot \boldsymbol{\sigma}, w) &= (f, w), \end{aligned} \tag{3.13}$$

for all $\mathbf{v} \in H_0(\text{div}, \Omega)$, and $w \in L^2(\Omega)/\mathbb{R}$. The lowest order Raviart–Thomas finite element space \mathcal{RT}_H is an $H_0(\text{div}, \Omega)$ -conforming discretization used for the flux space on the mesh \mathcal{T}_H . For the pressure space, we use the space of elementwise constants.

A multiscale method based on this discretization for Poisson’s equation on mixed form was proposed in [30], where also a posteriori error bounds were derived and used in an adaptive refinement algorithm. One observation from that work is that only a multiscale space for the flux needs to be constructed to be able to compute accurate solutions independent of fine scale variations. The coarse elementwise constant space can be left intact. Essentially the same method (however with a slightly different localization) is studied in Paper III, where we derive an a priori error bound for $\boldsymbol{\sigma}$, independent of the regularity of $\boldsymbol{\sigma}$ and u .

A practical implementation of the method is based on a discrete full space \mathcal{RT}_h (rather than $H(\text{div}, \Omega)$) with very small mesh size h , resolving the fine scale variations. The projection operator $\Pi_H : \mathcal{RT}_h \rightarrow \mathcal{RT}_H$ suffers from a mild L^2 -instability (with respect to $h \rightarrow 0$), for $\mathbf{v}_h \in \mathcal{RT}_h$ with $\nabla \cdot \mathbf{v}_h = 0$,

$$\|\Pi_H \mathbf{v}_h\|_{L^2(T)}^2 \leq C\lambda(H/h)^2 \|\mathbf{v}_h\|_{L^2(T)}^2,$$

where $\lambda(H/h) := (1 + \log(H/h))^{1/2}$ (see [42] for a proof). This affects the the final error bound for the flux $\boldsymbol{\sigma}_k^{\text{ms}}$ in the localized method,

$$\|A^{-1/2}(\boldsymbol{\sigma}_h - \boldsymbol{\sigma}_k^{\text{ms}})\|_{L^2(\Omega)} \leq C(H + k^{d/2}\lambda(H/h)^2\theta^{k/\lambda(H/h)})\|f\|_{L^2(\Omega)} \quad (3.14)$$

for some $0 < \theta < 1$ and C depending on the contrast, but not on k , h and H or the regularity of $\boldsymbol{\sigma}$ or u . The instability can be compensated by increasing the patch size k . For the non-localized method, the instability function does not enter the bound at all. The effect of the instability in the localized method, and its absence in the non-localized method, are observed in the numerical experiments. There exist Clément type interpolation operators [1, 9, 13] for which $\lambda = 1$ above. The paper [13] is particularly interesting from a computational point of view, since it constructs interpolation operators possessing a necessary commuting property based on local projections. However, this result was unknown to the authors of Paper III at the time it was written, and no numerical experiments using the operator were performed.

4. Estimating failure probabilities

In this chapter we study the problem of point estimation of the cumulative distribution function (cdf) for a random variable X that is an output from a model with random input ω . We assume that the model can not be evaluated exactly, but that approximations at different levels of accuracy can be computed. More precisely, the problem is to find the failure probability p for a critical value y of X ,

$$p = \Pr(X \leq y), \quad (4.1)$$

or equivalently, $p = F(y)$ where F is the cdf of X . The inverse problem, to determine quantile y from p is discussed in Paper V. However, since the main contribution in that paper (selective refinement) is more easily described in the context of estimating p , we focus on that case here. The idea of selective refinement is to use error estimates for approximate realizations of X and refine only realizations that can possibly affect the estimate of p , thereby avoiding unnecessary computational work.

In the context of the two-phase Darcy flow model presented in Chapter 2, the random input ω is the uncertain permeability field K and X is a functional of the solutions σ_β , s_β and u_β . We will call this functional the quantity of interest. One example of a quantity of interest is the flux over a segment $\Gamma \subset \partial\Omega$ of the domain boundary. This flux can be expressed as the integral

$$X = \int_\Gamma \boldsymbol{\sigma} \cdot \mathbf{n}, \quad (4.2)$$

where \mathbf{n} is the outward unit normal vector of Γ . Another example is sweep efficiency, which is the fraction of the domain Ω that has been swept by, for instance the non-wetting phase, at a final time T , i.e.

$$X = |\Omega|^{-1} \int_\Omega \chi_{(0,1]}(s_n(T)), \quad (4.3)$$

where χ_A is the indicator function for the set A . Throughout this work we consider the distribution of ω as given and that it can be sampled.

The selective refinement method is applicable to stochastic integration methods for estimating expected values. Failure probabilities can be estimated by introducing the binary variable $Q = \chi_{(-\infty, y]}(X)$ and computing

$$p = \mathbb{E}[Q], \quad (4.4)$$

where $\mathbb{E}[\cdot]$ denotes expected value. Note that Q attains only the values 1 and 0 with probability p and $1 - p$, respectively. This means there are discontinuities in Q with respect to the stochastic variables. Hence, methods exploiting smoothness or low variation of the integrand, such as sparse grids [39, 15], lattice rules [38] and quasi-Monte Carlo [32] are not expected to perform optimally in general. The works in this thesis are based on Monte Carlo and multilevel Monte Carlo [16, 20] methods. The following sections summarize Papers IV–VI.

4.1 Monte Carlo

We introduce a hierarchy X_ℓ , $\ell = 0, 1, 2, \dots$ of approximations of X that satisfy the max-norm bound

$$|X - X_\ell| \leq \gamma^\ell, \quad (4.5)$$

for a $0 < \gamma < 1$. The approximate failure probability $Q_\ell = \chi_{(-\infty, y]}(X_\ell)$ can be sampled to estimate an approximate failure probability $p_\ell = \mathbb{E}[Q_\ell]$. If $\{Q_L^i\}_{i=1}^N$ is an independent sample with the same distribution as Q_L , then the Monte Carlo estimator for an approximation at level $\ell = L$ is

$$\widehat{Q}_{N,L}^{\text{MC}} = \frac{1}{N} \sum_{i=1}^N Q_L^i.$$

To measure the error, we use the mean squared error, which can be split into two terms, separating the sampling error and the numerical bias,

$$e \left[\widehat{Q}_{N,L}^{\text{MC}} \right]^2 = \mathbb{E} \left[(\widehat{Q}_{N,L}^{\text{MC}} - \mathbb{E}[Q])^2 \right] = N^{-1} \text{Var}[Q_L] + (\mathbb{E}[Q_L - Q])^2, \quad (4.6)$$

where $\text{Var}[\cdot]$ denotes the variance. We wish this error to be less than ε^2 and require that $(\mathbb{E}[Q_L - Q])^2 \leq \frac{1}{2}\varepsilon^2$ and $N^{-1} \text{Var}[Q_L] \leq \frac{1}{2}\varepsilon^2$, i.e. that the error sources contribute equally. The bias can be bounded by the assumed max-norm error of X_ℓ and the Lipschitz constant C_F of F ,

$$\mathbb{E}[Q_L - Q] \leq \Pr(|X - y| \leq \gamma^L) = F(y + \gamma^L) - F(y - \gamma^L) \leq 2C_F \gamma^L.$$

Thus, we should pick $L \approx \log_\gamma(\varepsilon)$ to get the desired accuracy. The variance of a Bernoulli distribution Q_L with parameter p_L is $\text{Var}[Q_L] = p_L(1 - p_L) \leq 1$, and the number of samples N is chosen proportional to ε^{-2} to obtain sufficiently small variance. In the limit $p \rightarrow 0$, for so called rare events, one wants a relative error $\varepsilon/p \leq 1$. We do not specifically address this situation here. See e.g. [2, 18, 19, 41] for methods applicable in that situation. Assuming the following cost model

$$\mathcal{C}[X_\ell] = \gamma^{-q\ell},$$

for some $q > 0$, where $\mathcal{C}[X_\ell]$ denotes the expected computational cost to compute a realization of X_ℓ , the total cost of the Monte Carlo estimator is

$$\mathcal{C}[\widehat{Q}_{N,L}^{\text{MC}}] = N\gamma^{-qL} \approx \varepsilon^{-2-q}.$$

We use the notation $a \lesssim b$ for $a \leq Cb$ for a constant C independent of ε and γ , and $a \approx b$ for $a \lesssim b \lesssim a$. One can think of the factors ε^{-2} and ε^{-q} as stemming from the aims to reduce the sampling error and numerical bias, respectively.

4.2 Multilevel Monte Carlo

The multilevel Monte Carlo (MLMC) method [16, 20] is a variance reduction technique that uses the full hierarchy Q_ℓ ($0 \leq \ell \leq L$) to estimate $\mathbb{E}[Q_L]$. It can be interpreted as a recursive application of control variates. A new random variable Z is formed using Q and an a priori known random variable R correlated with Q and with known expected value:

$$Z = \mathbb{E}[R] + Q - R.$$

The variance $\text{Var}[Z] = \text{Var}[Q - R]$ is smaller than $\text{Var}[Q]$ if Q and R are sufficiently correlated. Now, Z (with lower variance) is sampled instead of Q . A smaller sample is needed to obtain the same variance of the estimator. For this to be beneficial, we need that (i) realizations of R are sufficiently cheap to generate and (ii) the expected value of R is known (or can be estimated). In the multilevel Monte Carlo method, less accurate and cheap approximations are used as control variates for more accurate and expensive approximations. We expand $\mathbb{E}[Q_L]$ in a telescoping sum of L levels (and level 0):

$$\mathbb{E}[Q_L] = \mathbb{E}[Q_0] + \sum_{\ell=1}^L \mathbb{E}[Q_\ell - Q_{\ell-1}]. \quad (4.7)$$

The expected values on the right hand side in (4.7) are estimated using standard MC estimators, with an individual sample size N_ℓ for each level ℓ :

$$\widehat{Q}_{\{N_\ell\},L}^{\text{ML}} = \frac{1}{N_0} \sum_{i=1}^{N_0} Q_0^i + \sum_{\ell=1}^L \frac{1}{N_\ell} \sum_{i=1}^{N_\ell} Y_\ell^i,$$

where $Y_\ell = Q_\ell - Q_{\ell-1}$ are called correctors. The cost estimate for MLMC depends on the rates with which the bias $\mathbb{E}[Q_\ell - Q]$ and the corrector variance $\text{Var}[Q_\ell - Q_{\ell-1}]$ converge with ℓ . Under assumption (4.5), the convergence rate for the bias is γ^ℓ according to the discussion in the previous section. See the related work [3] for bounds of the expectation of $Q_\ell - Q$ given weaker moments of $X_\ell - X$. In addition to q , we assume that there is a constant $b \leq 2$, so that we have

$$\begin{aligned} |\mathbb{E}[Q_\ell - Q]| &\lesssim \gamma^\ell, \\ \text{Var}[Q_\ell - Q_{\ell-1}] &\lesssim \gamma^{b\ell}, \text{ for } \ell \geq 1. \end{aligned}$$

The sample sizes N_ℓ are determined by minimizing the expected cost with constraint that the variance of the estimator is equal to ε^2 . Now if the deepest level L is chosen to balance the numerical bias with the sampling error (as in the Monte Carlo case), we obtain three cases for the expected cost [16],

$$C \left[\widehat{Q}_{\{N_\ell\},L}^{\text{ML}} \right] \lesssim \begin{cases} \varepsilon^{-2} & q < b, \\ \varepsilon^{-2} (\log \varepsilon^{-1})^2 & q = b, \\ \varepsilon^{-2-q+b} & q > b. \end{cases}$$

For quantities of interests computed from numerical solutions of PDEs, we are typically in the case $q > b$. Optimally, the variance converges with the double rate compared to that of the bias, i.e. $b = 2$. If this is the case, it is possible to get a reduction in computational cost by a factor ε^2 compared to Monte Carlo. This is, however, not the case for the failure probability functional Q , where the rates can be shown to be equal, i.e. $b = 1$. In [17], smoothness of F is exploited to regain the optimal rate by proper smoothing of χ . In this work, we use the max-norm error estimate (4.5) and construct an algorithm to regain the optimal rate by reducing the expected cost of each realization.

4.3 Selective refinement

We replace the assumption (4.5) with the weaker assumption

$$|X - X_\ell| \leq \gamma^\ell \quad \text{or} \quad |X - X_\ell| < |X_\ell - y| \quad (4.8)$$

(see Figure 4.1) and instead introduce X'_k that we assume satisfy (4.5)

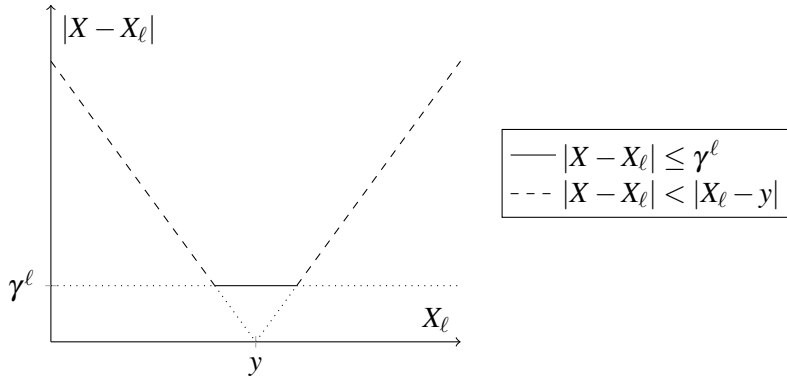


Figure 4.1. Illustration of condition (4.8). The numerical error is allowed to be larger than γ^ℓ far away from y .

$$|X - X'_k| \leq \gamma^k, \quad (4.9)$$

Algorithm 1 Selective refinement algorithm to compute X_ℓ

- 1: Compute X'_0
 - 2: Let $k = 0$
 - 3: **while** $k < \ell$ and $|X'_k - y| \leq \gamma^k$ **do**
 - 4: Let $k = k + 1$
 - 5: Compute X'_k
 - 6: **end while**
 - 7: Let $X_\ell = X'_k$
-

with $\mathcal{C}[X'_k] = \gamma^{-kq}$ as in the previous sections. Under these assumptions, it is possible to compute X_ℓ by the algorithm in Algorithm 1. We note that the number of iterations in the selective refinement algorithm depends on the particular realization and is thus itself a random variable. The algorithm has computational complexity $\mathcal{C}[X_\ell] \leq C\gamma^{-\ell(q-1)}$, where C depends on probability density close to y (or in worst case Lipschitz constant C_F of F). If using this algorithm to compute X_ℓ , the results from the previous sections (again with $b = 1$) are applicable with q replaced by $q - 1$, and we regain the the optimal rate for large q ,

$$\mathcal{C}[\widehat{Q}_{\{N_\ell\},L}^{\text{ML}}] \lesssim \begin{cases} \varepsilon^{-2} & q < 2, \\ \varepsilon^{-2}(\log \varepsilon^{-1})^2 & q = 2, \\ \varepsilon^{-q} & q > 2. \end{cases}$$

The error bound (4.9) can be difficult to derive, since it needs to hold with probability one. In a practical situation, however, it might be possible to motivate a probabilistic bound that is broken only with a probability α ,

$$\Pr(|X - X'_k| \leq \gamma^k) \geq 1 - \alpha, \quad (4.10)$$

for each k separately. This adds a bias to $\mathbb{E}[Q_\ell - Q]$ smaller than $(\ell + 1)\alpha$, so that

$$\begin{aligned} |\mathbb{E}[Q_\ell - Q]| &\lesssim \gamma^\ell + (\ell + 1)\alpha, \\ \text{Var}[Q_\ell - Q_{\ell-1}] &\lesssim \gamma^\ell + (\ell + 1)\alpha, \text{ for } \ell \geq 1. \end{aligned} \quad (4.11)$$

Thus, if for a given deepest level L we pick $\alpha \lesssim (L + 1)^{-1}\varepsilon \lesssim (L + 1)^{-1}\gamma^\ell$, it is still possible to apply the computational complexity results above. In Paper VI, we apply the selective refinement algorithm to a Darcy flow problem to estimate the probability for the sweep efficiency X to be below a certain critical value y . The number of discretization levels L was fixed to 4, and the accuracy ε was in the order of 1 %, allowing for an $\alpha \approx 10^{-3}$. The numerical results showed that selective refinement can reduce the computational cost by a factor of 5–10 in a practical example compared to multilevel and standard Monte Carlo. The bias $(\ell + 1)\alpha$ from the probabilistic bound can be reduced to α under the assumption that the bound (4.10) holds independently of the (random) number of iterations in the selective refinement algorithm.

5. Summary of papers

5.1 Paper I

F. Hellman and A. Målqvist. Contrast independent localization of multiscale problems. *ArXiv e-prints:1610.07398*, 2016.

The error from localization of element correctors in the LOD method is contrast dependent for general choices of interpolation operators. We study an elliptic problem with a coefficient taking one of only two possible values α and 1, with $\alpha \ll 1$. We partition Ω into two disjoint subdomains Ω^1 and Ω^α based on the value of A so that $A|_{\Omega^\alpha} = \alpha$ and $A|_{\Omega^1} = 1$. This allows for a geometrical interpretation of the coefficient in terms of the subdomains Ω^α and Ω^1 . We propose an interpolation operator defined in terms of the geometry of Ω^1 that gives contrast independent localization error. The construction puts some conditions on the placement of coarse nodes in relation to the geometry of Ω^1 . The implications of these conditions are studied.

Contributions

The author of this thesis had the main responsibility for preparing the manuscript, performed all the numerical experiments and performed most of the analysis. The ideas were developed in close collaboration with the other author.

5.2 Paper II

F. Hellman and A. Målqvist. Numerical homogenization of time-dependent diffusion. *ArXiv e-prints:1703.08857*, 2017.

We study the LOD method for a sequence of elliptic problems with similar rapidly varying coefficients. These occur for example in sample based stochastic integration or in splitting schemes for time-dependent problems. We define a method that constructs a multiscale space for the first coefficient in the sequence and then adaptively updates the element correctors while stepping through the sequence. Computable error indicators are used to tell which element correctors to recompute in order to keep the error below a predetermined tolerance throughout the sequence of PDEs. The method automatically exploits the decay of the element correctors to only make the necessary updates.

Contributions

The author of this thesis had the main responsibility for preparing the manuscript, performed all the numerical experiments and performed most of the analysis. The ideas were developed in close collaboration with the other author.

5.3 Paper III

F. Hellman, P. Henning, and A. Målqvist. Multiscale mixed finite elements. *Discrete Contin. Dyn. Syst. Ser. S*, 9(5):1269–1298, 2016.

In this paper we derive an a priori error bound for the LOD method on Poisson’s equation on mixed form, based on the Raviart–Thomas finite element. We observe that it is only necessary to construct a low-dimensional multiscale space for the flux variable (i.e. the pressure variable needs no modification) to get a regularity independent error bound for the flux. The flux solution is also conservative on the coarse mesh and can be made conservative on the fine mesh if using right hand side correction. The error bound, however, grows logarithmically with H/h due to the L^2 -instability of the standard Raviart–Thomas interpolation. Clément type interpolation operators can be used to remove this instability.

Contributions

The author of this thesis had the main responsibility for preparing the manuscript, performed all the numerical experiments and performed parts of the analysis. The ideas were developed in close collaboration with the other authors.

5.4 Paper IV

D. Elfverson, D. Estep, F. Hellman, and A. Målqvist. Uncertainty quantification for approximate p -quantiles for physical models with stochastic inputs. *SIAM/ASA J. Uncertain. Quantif.*, 2(1):826–850, 2014.

We develop a method for estimating p -quantiles y for outputs from a computational model with random inputs. Using computable error bounds for the numerical error and confidence bands for the sampling error, we propose an algorithm for computing computable lower and upper bounds, $y_{n,\varepsilon}^-$ and $y_{n,\varepsilon}^+$, respectively, so that

$$\Pr(y_{n,\varepsilon}^- \leq y \leq y_{n,\varepsilon}^+) \geq 1 - \beta,$$

given a (small) probability $0 < \beta < 1$. The algorithm (called selective refinement) exploits that the accuracy of only a subset of the realizations affects the accuracy of the estimator to reduce the computational cost. We also analyze

the asymptotic convergence properties of the p -quantile estimator bounds in the limit of large sample size and decreasing numerical error.

Contributions

The author of this thesis wrote the manuscript and performed the numerical experiments in close collaboration with the first author. The analysis was done by the author of this thesis, the first, and the fourth author. The ideas were developed in close collaboration between all the authors.

5.5 Paper V

D. Elfverson, F. Hellman, and A. Målqvist. A multilevel Monte Carlo method for computing failure probabilities. *SIAM/ASA J. Uncertain. Quantif.*, 4(1): 312–330, 2016.

We develop a multilevel Monte Carlo method for estimating failure probabilities $p = \Pr(X \leq y)$ for a given critical value y , where X is the output from a model with random input. Using max-norm error bounds for the error in a hierarchy of increasingly expensive and accurate approximations X_ℓ , $\ell = 0, 1, \dots$ of X , we define an algorithm that reduces the cost complexity in terms of the desired accuracy for the multilevel Monte Carlo method. The algorithm exploits that the accuracy of only a subset of the realizations affects the accuracy of the estimator. This makes it possible to compute only a fraction of all realizations using the most accurate approximation. We prove that the asymptotic cost in the limit of root mean square error tolerance $\varepsilon \rightarrow 0$ is proportional to that of computing a single approximation on the most accurate level in the hierarchy.

Contributions

The author of this thesis wrote the manuscript, performed the numerical experiments and did the analysis in close collaboration with the first author. The ideas were developed in close collaboration with all the authors.

5.6 Paper VI

F. Fagerlund, F. Hellman, A. Målqvist, and A. Niemi. Multilevel Monte Carlo methods for computing failure probability of porous media flow systems. *Advances in Water Resources*, 94:498–509, 2016.

In this paper we consider a two-phase Darcy flow system simulating an injection scenario and estimate the probability for the sweep efficiency of the injected fluid to be less than a predetermined critical value, given a probabilistic model for the permeability. We use the selective refinement technique from

Papers IV–V in combination with standard Monte Carlo and multilevel Monte Carlo to reduce the computational cost. Cost reductions of magnitude 5–10 are observed. We also discuss heuristics for estimating parameters required by the methods and derive an error bound for the error introduced by using a probabilistic bound for the approximation errors instead of the max-norm bound assumed by the method in Paper V.

Contributions

The author of this thesis had the main responsibility for preparing the manuscript and performed all computations and analysis. The ideas were developed in collaboration between all authors.

6. Sammanfattning på svenska

Darcys lag är en modell som beskriver hur vätskor och gaser flödar i porösa material. Det är kanske den modell som används mest i storskaliga datorsimuleringar av underjordiska flöden, exempelvis spridning av föroreningar i grundvatten, olje- och vattenflöden i oljereservoarer för utökad oljeutvinning och flöden av saltvatten och koldioxid i salina akvifärer för koldioxidlagring. Denna avhandling tar upp två stora utmaningar för sådana datorsimuleringar: (i) att materialegenskaperna varierar med stor kontrast och på mycket mindre skala än skalan på området som beräkningen rör (snabbt varierande data) och (ii) att materialegenskaperna till stor del är okända (osäker data). Problem med osäker och snabbt varierande data förekommer i många andra situationer, till exempel vid simuleringar för kompositmaterial. Trots att många av resultaten i denna avhandling också är tillämpbara på andra problem, diskuterar vi resultaten i ett sammanhang av underjordiska flöden för att visa på en viktig tillämpning.

För ett Darcy-flödesproblem tar ekvationen för trycket u ofta formen av en elliptisk partiell differentialekvation (PDE)

$$-\nabla \cdot A \nabla u = f,$$

där f är käll- och sänktermer och koefficienten A är kopplad till permeabiliteten. Permeabiliteten avgör i vilken grad en vätska eller gas kan flöda genom en viss punkt i området och den kan variera betydligt över korta avstånd på grund av lokala variationer i berggrundens egenskaper. Den kan också variera med flera storleksordningar när material med vitt skilda egenskaper förekommer inom beräkningsområdet. Finita elementmetoden är en vanlig metod för att lösa elliptiska ekvationer. I fallet med snabbt varierande koefficienter måste dock beräkningsnätet lösa upp de fina variationerna i A för att metoden ska ge en noggrann lösning. Ett fint nät gör att det resulterande linjära ekvations-systemet blir mycket stort och en snabbt varierande koefficient gör det även svårt att lösa med iterativa metoder [7, 12]. För att kunna göra storskaliga simuleringar behöver vi minneseffektiva och parallelliserbara algoritmer.

Numerisk homogenisering eller multiskalmetoder behandlar problemet med snabbt varierande koefficienter. En vanligt förekommande strategi är att lösa små lokaliserade problem, vars lösning används för att konstruera en uppskalad operator eller modifierade basfunktioner på ett grövre nät, som sedan ger bättre grovskaliga approximationer. I denna avhandling studerar vi lokaliserade ortogonaluppdelningsmetoden (LOD, [27, 29]), som har sina rötter

i variationsmultiskalmetoden (VMS, [24]). LOD är en parallelliserbar metod för att konstruera ett lågdimensionellt multiskalrum utifrån koefficienten A med bevisbart goda approximationsegenskaper. Detta står i kontrast mot de vanliga finita elementrummen, där man alltid kan hitta en koefficient sådan att metoden konvergerar godtyckligt långsamt [5]. Två nära besläktade multiskalmetoder är multiskal-finita elementmetoden [22] och nätfri polyharmonisk homogenisering [33]. Konvergensanalysen för multiskal-finita elementmetoden bygger dock på att A är periodisk. Nätfri polyharmonisk homogenisering kan tillämpas under svagare antaganden och de numeriska experimenten visar att lokalisering är möjlig med bibehållen noggrannhet även för denna metod.

Vi fokuserar på tre aspekter av LOD. En aspekt är koefficienter med hög kontrast, d.v.s. stort förhållande mellan största och minsta värde av A . Kontrasten ingår i feluppskattningarna för vanliga LOD som en konstant och begränsar möjligheten till lokalisering. Vi gör det förenklande antagandet att A är lika med antingen α eller 1 i varje punkt, vilket tillåter en geometrisk tolkning av koefficienten. Vi föreslår en modifiering av LOD för kontrastoberoende lokalisering. En annan aspekt är tidsvarierande koefficienter som förekommer till exempel i tidsberoende tvåfas-Darcy-flödesproblem. Här konstruerar vi ett initialt multiskalrum och härleder felindikatorer som kan tala om när och var vi behöver uppdatera multiskalrummet för att hålla felet nere när vi stegar i tiden. Slutligen tillämpar vi LOD på mixade finita element, mer specifikt på Raviart–Thomas-elementet. Vi härleder a priori-feluppskattningar oberoende av de finskaliga variationerna och erhåller en lösning som är lokalt konservativ.

Koefficienten A i tryckekvationen ovan är typiskt inte bara snabbt varierande, utan även osäker. Detta har motiverat oss att utveckla och analysera metoder för fortplantning av osäkerhet. Problemformuleringen är allmän. Vi betraktar utdata X från en modell med slumpmässig indata ω och vi är intresserade av att uppskatta felrisken $p = F(y)$, där F är den kumulativa distributionsfunktionen av X . Med andra ord, storheten X indikerar på ett fel om $X \leq y$ och p är sannolikheten för detta att inträffa. Metoder för denna typ av problem innefattar de som konstruerar en representation av X i det stokastiska rummet, t.ex. första/andra ordningens pålitlighetsmetoder (FORM/SORM) [26] och surrogatbaserade metoder (t.ex. [28]). De förstnämnda kan inte förväntas prestera bra om det inte finns något känt normaltillstånd från vilket en gränspunkt för fel kan bestämmas. De senare lider av dimensionalitetens förbannelse. Detta kan vara kritiskt för underjordiska flödesproblem där den slumpmässiga indatan ofta är ett spatiellt slumpfält av hög stokastisk dimension. Det finns även stickprovsbaserade metoder specifikt konstruerade för att beräkna felrisiker, t.ex. delmängdssimulering [2, 41], där Markovkedje-Monte Carlo-tekniker används för att generera stickprov koncentrerade till felhändelsen.

I denna avhandling betraktar vi stickprovsbaserade metoder för stokastisk integrering. Vi fokuserar på Monte Carlo- och flernivå-Monte Carlo-metoder

[16] som är oberoende av representationen hos den slumpmässiga indatan. Resultaten här är dock användbara också i kombination med kvasi-Monte Carlo-metoder, gittermetoder och glesa nät, om regulariteten tillåter någon vinst av att använda dessa. Vi betraktar det typiska fallet att enbart numeriska approximationer av X är tillgängliga och att vi har möjlighet att beräkna approximationer X_ℓ för vilka felet $|X - X_\ell|$ avtar exponentiellt med ℓ . Vi använder beräkningsbara begränsningar på felet för att hitta delmängder av realisationer att beräkna på lägre approximationsnivåer och på så sätt uppnå förbättrad komplexitetsordning för beräkningskostnaden jämfört med den vanliga Monte Carlo-metoden och flernivå-Monte Carlo-metoden.

De tre kapitlen 2–4 ger en mer detaljerad sammanfattning av de ingående arbetena. Kapitel 2 beskriver en modell för Darcy-flödesproblemet. Denna modell återkommer i numeriska experiment och exempel i flera av artiklarna. Kapitel 3 tar upp ämnet om numerisk homogenisering som täcks av artiklarna I–III och kapitel 4 behandlar arbetet på felriskuppskattningar som finns i artiklarna IV–VI.

Acknowledgments

First of all, I want to thank my main adviser Axel Målqvist for your invaluable support over the past five years. I have greatly appreciated your sincere interest in my development as a researcher. I am particularly grateful that you have shared with me your excellent view on computational mathematics. I would also like to thank my co-advisers Auli Niemi and Fritjof Fagerlund for sharing your expertise in hydrogeology and teaching me about flows in porous media. In addition to my advisers, I want to thank my other co-authors Daniel Elfverson, Donald Estep, and Patrick Henning for your great contributions to our joint efforts and for all the fun it has been working together. I would also like to thank Daniel Peterseim, Knut-Andreas Lie, and Elisabeth Ullmann for good discussions providing me with additional and valuable insights. It is impossible to deny that the early opportunities given to me by Kenneth Holmström set me off on the path to this thesis. For this I am very grateful.

I thank the Centre for Interdisciplinary Mathematics, Uppsala University for funding this thesis work. I am also grateful for generous travel grants from Anna Maria Lundins stipendiefond, Ångpanneföreningens forskningsstiftelse, C. F. Liljewalchs stipendiestiftelse, C. Swartz' stiftelse, and H. F. Sederholms stipendiestiftelse.

I have really enjoyed the friendly atmosphere at TDB and want to thank all friends and colleagues there. So many nice people, so close to my desk. In my view, a very good arrangement. Thank you all for making it a pleasure to go to work! Special thanks to Martin Almquist for providing valuable comments on a draft of this summary and for the help during the last few weeks.

To my friends, thank you for offering good advice and support during this time. Special thanks to Olof Jönsson, David Berglund, Mikael Thuné, Ian Wainwright, Josefin Ahlkrona, Martin Almquist, Daniel Elfverson, Patrick Henning, Hanna Holmgren, Kalle Ljungkvist, Lina Meinecke, Slobodan Milovanović, Simon Sticko, Martin Tillenius, and Emil Nordling.

Slutligen, stort tack till mamma, Anna och Åsa för allt. Jag är så glad att jag har er!

References

- [1] D. N. Arnold, R. S. Falk, and R. Winther. Finite element exterior calculus, homological techniques, and applications. *Acta Numer.*, 15:1–155, 2006.
- [2] S.-K. Au and J. L. Beck. Estimation of small failure probabilities in high dimensions by subset simulation. *Probabilistic Engineering Mechanics*, 16(4):263–277, 2001.
- [3] R. Avikainen. On irregular functionals of SDEs and the Euler scheme. *Finance Stoch.*, 13(3):381–401, 2009.
- [4] I. Babuška and J. E. Osborn. Generalized finite element methods: Their performance and their relation to mixed methods. *SIAM J. Numer. Anal.*, 20(3):510–536, 1983.
- [5] I. Babuška and J. E. Osborn. Can a finite element method perform arbitrarily badly? *Math. Comp.*, 69(230):443–462, 2000.
- [6] A. Bensoussan, J. L. Lion, and G. Papanicolaou. *Asymptotic Analysis for Periodic Structure*, volume 5 of *Studies in Mathematics and Its Applications*. North-Holland, Amsterdam, 1978.
- [7] L. V. Branets, S. S. Ghai, S. L. Lyons, and X.-H. Wu. Challenges and technologies in reservoir modeling. *Commun. Comput. Phys.*, 6(1):1–23, 2009.
- [8] S. C. Brenner and L. R. Scott. *The Mathematical Theory of Finite Element Methods*, volume 15 of *Texts in Applied Mathematics*. Springer, New York, 3rd edition, 2008.
- [9] S. H. Christiansen and R. Winther. Smoothed projections in finite element exterior calculus. *Math. Comp.*, 77(262):813–829, 2008.
- [10] P. Ciarlet. *The Finite Element Method for Elliptic Problems*. North-Holland, Amsterdam, 1978.
- [11] Ph. Clément. Approximation by finite element functions using local regularization. *ESAIM: Mathematical Modelling and Numerical Analysis - Modélisation Mathématique et Analyse Numérique*, 9(2):77–84, 1975.
- [12] B. Engquist and E. Luo. Convergence of a multigrid method for elliptic equations with highly oscillatory coefficients. *SIAM J. Numer. Anal.*, 34(6):2254–2273, 1997.
- [13] R. S. Falk and R. Winther. Local bounded cochain projections. *Math. Comp.*, 83:2631–2656, 2014.
- [14] L. W. Gelhar. *Stochastic Subsurface Hydrology*. Prentice Hall, New Jersey, 1993.
- [15] T. Gerstner and M. Griebel. Numerical integration using sparse grids. *Numer. Algorithms*, 18(3–4):209–232, 1998.
- [16] M. B. Giles. Multilevel Monte Carlo path simulation. *Oper. Res.*, 56(3):607–617, 2008.
- [17] M. B. Giles, T. Nagapetyan, and K. Ritter. Multilevel Monte Carlo approximation of distribution functions and densities. *SIAM/ASA J. Uncertain. Quantif.*, 3(1):267–295, 2015.

- [18] P. Glasserman, P. Heidelberger, P. Shahabuddin, and T. Zajic. Splitting for rare event simulation: Analysis of simple cases. In *Proceedings of the 1996 Winter Simulation Conference*, pages 302–308, 1996.
- [19] P. Glynn. Importance sampling for Monte Carlo estimation of quantiles. In *Mathematical Methods in Stochastic Simulation and Experimental Design: Proc. 2nd St. Petersburg Workshop on Simulation (Publishing House of Saint Petersburg University)*, pages 180–185, 1996.
- [20] S. Heinrich. Multilevel Monte Carlo methods. In *Large-Scale Scientific Computing*, volume 2179 of *Lecture Notes in Computer Science*, pages 58–67. Springer Berlin Heidelberg, 2001.
- [21] P. Henning and A. Målqvist. Localized orthogonal decomposition techniques for boundary value problems. *SIAM J. Sci. Comput.*, 36(4):A1609–A1634, 2014.
- [22] T. Y. Hou and X.-H. Wu. A multiscale finite element method for elliptic problems in composite materials and porous media. *J. Comput. Phys.*, 134(1):169 – 189, 1997.
- [23] T.Y. Hou, X.-H. Wu, and Z. Cai. Convergence of a multiscale finite element method for elliptic problems with rapidly oscillating coefficients. *Math. Comp.*, 68:913–943, 1999.
- [24] T. J. R. Hughes, G. R. Feijóo, L. Mazzei, and J.-B. Quinicy. The variational multiscale method—a paradigm for computational mechanics. *Comput. Methods Appl. Mech. Engrg.*, 166(1-2):3–24, 1998.
- [25] T. J. R. Hughes and G. Sangalli. Variational multiscale analysis: The fine-scale Green’s function, projection, optimization, localization, and stabilized methods. *SIAM J. Numer. Anal.*, 45(2):539–557, 2007.
- [26] A. Der Kiureghian. First- and second-order reliability methods. In E. Nikolaidis, D. M. Ghiocel, and S. Singhal, editors, *Engineering Design Reliability Handbook*, chapter 14. CRC Press, Boca Raton, FL, 2005.
- [27] M. G. Larson and A. Målqvist. Adaptive variational multiscale methods based on a posteriori error estimation: Energy norm estimates for elliptic problems. *Comput. Methods Appl. Mech. Engrg.*, 196:2313–2324, 2007.
- [28] Jing Li, Jinglai Li, and D. Xiu. An efficient surrogate-based method for computing rare failure probability. *J. Comput. Phys.*, 230(24):8683 – 8697, 2011.
- [29] A. Målqvist and D. Peterseim. Localization of elliptic multiscale problems. *Math. Comp.*, 83(290):2583–2603, 2014.
- [30] A. Målqvist. Multiscale methods for elliptic problems. *Multiscale Model. Simul.*, 9(3):1064–1086, 2011.
- [31] J. C. Nedelec. Mixed finite elements in \mathbb{R}^3 . *Numerische Mathematik*, 35(3):315–341, 1980.
- [32] H. Niederreiter. *Random Number Generation and Quasi-Monte Carlo Methods*. SIAM, Philadelphia, 1992.
- [33] Owahdi, H., Zhang, L., and Berlyand, L. Polyharmonic homogenization, rough polyharmonic splines and sparse super-localization. *ESAIM: M2AN*, 48(2):517–552, 2014.
- [34] D. Peterseim. Variational multiscale stabilization and the exponential decay of fine-scale correctors. In G. R. Barrenechea, F. Brezzi, A. Cangiani, and E. H.

- Georgoulis, editors, *Building Bridges: Connections and Challenges in Modern Approaches to Numerical Partial Differential Equations*, Lecture Notes in Computational Science and Engineering. Springer, May 2016.
- [35] D. Peterseim and R. Scheichl. Robust numerical upscaling of elliptic multiscale problems at high contrast. *Comput. Meth. in Appl. Math.*, 16(4):579–603, 2016.
- [36] P. A. Raviart and J. M. Thomas. A mixed finite element method for 2-nd order elliptic problems. In Ilio Galligani and Enrico Magenes, editors, *Mathematical Aspects of Finite Element Methods*, volume 606 of *Lecture Notes in Mathematics*, pages 292–315. Springer Berlin Heidelberg, 1977.
- [37] L. R. Scott and S. Zhang. Finite element interpolation of nonsmooth functions satisfying boundary conditions. *Math. Comp.*, 54(190):483–493, 1990.
- [38] I. H. Sloan and S. Joe. *Lattice methods for multiple integration*. Oxford University Press, Oxford, 1994.
- [39] S. A. Smolyak. Quadrature and interpolation formulas for tensor products of certain classes of functions. *Dokl. Akad. Nauk*, 4:240–243, 1963.
- [40] S. Sun and J. Liu. A locally conservative finite element method based on piecewise constant enrichment of the continuous Galerkin method. *SIAM J. Sci. Comput.*, 31(4):2528–2548, 2009.
- [41] E. Ullmann and I. Papaioannou. Multilevel estimation of rare events. *SIAM/ASA J. Uncertain. Quantif.*, 3(1):922–953, 2015.
- [42] B. Wohlmuth, A. Toselli, and O. Widlund. An iterative substructuring method for Raviart–Thomas vector fields in three dimensions. *SIAM J. Numer. Anal.*, 37(5):1657–1676, 2000.

Acta Universitatis Upsaliensis

*Digital Comprehensive Summaries of Uppsala Dissertations
from the Faculty of Science and Technology 1495*

Editor: The Dean of the Faculty of Science and Technology

A doctoral dissertation from the Faculty of Science and Technology, Uppsala University, is usually a summary of a number of papers. A few copies of the complete dissertation are kept at major Swedish research libraries, while the summary alone is distributed internationally through the series Digital Comprehensive Summaries of Uppsala Dissertations from the Faculty of Science and Technology. (Prior to January, 2005, the series was published under the title “Comprehensive Summaries of Uppsala Dissertations from the Faculty of Science and Technology”.)

Distribution: publications.uu.se
urn:nbn:se:uu:diva-318589



ACTA
UNIVERSITATIS
UPSALIENSIS
UPPSALA
2017